

SLC INJECTOR SIMULATION AND TUNING FOR HIGH CHARGE TRANSPORT*

A. D. Yeremian, R. H. Miller, J. E. Clendenin, R. A. Early, M. C. Ross, J. L. Turner, J. W. Wang
Stanford Linear Accelerator Center
Stanford Ca. 94309

Abstract

We have simulated the SLC injector from the thermionic gun through the first accelerating section and used the resulting parameters to tune the injector for optimum performance and high charge transport.

Simulations are conducted using PARMELA, a three-dimensional ray-trace code with a two-dimensional space-charge model. The magnetic field profile due to the existing magnetic optics is calculated using POISSON, while SUPERFISH is used to calculate the space harmonics of the various bunchers and the accelerator cavities. The initial beam conditions in the PARMELA code are derived from the EGUN model of the gun. The resulting injector parameters from the PARMELA simulation are used to prescribe experimental settings of the injector components.

The experimental results are in agreement with the results of the integrated injector model.

Introduction

The purpose of the SLC injector is to deliver two bunches of electrons to the damping ring at 1.2 GeV. The bunches of electrons are 61 ns apart, with greater than 6×10^{10} electrons, in 20 ps per bunch, at the repetition rate of up to 120 Hz, with less than 2% intensity jitter.

The SLC injector was designed ten years ago, using a one-dimensional, longitudinal, bunching code [1]. Although the injector has been operating reasonably satisfactorily since that time, to meet the requirements for steady, high-current operation we have modeled the entire injector in a consistently integrated way, using various codes of two or more dimensions for each portion, to improve its performance.

This paper will address the modeling from the gun to the 40 MeV point in detail, followed by a discussion of experimental techniques used to achieve the high-current operation of the injector.

Injector Simulation

The SLC injector consists of two electron guns, each at a 38° angle from the accelerator centerline; a switching magnet to allow the operation of either gun; a bunching section consisting of two subharmonic bunchers (SHB) at 178.5 MHz separated by 108 cm; a 4-cell, $\beta = .75$ S-band (2856 MHz) buncher; and a 3m, traveling-wave, S-band accelerating section with $\beta = 1$, which contributes to bunching as well as accelerating the beam to 40 MeV. The injector compresses the

2.5 ns bunch from the gun to 20 ps at 40 MeV. Beyond 40 MeV there are a series of accelerating sections to accelerate the beam to 1.2 GeV. The radial growth of the beam due to space charge is controlled by the axial magnetic fields provided by the lenses, solenoids and field-shaping iron up to 40 MeV and quadrupoles beyond that. The diagnostic devices to aid in tuning and characterizing the beam consist of beam position monitors (BPM), fast-wall-gap current monitors, a bunching monitor, energy and energy-spread analyzing stations at 0.04, 0.2, and 1.2 GeV, beam-loss monitors, fluorescent screen-beam profile monitors at 40 and 80 MeV, and wire scanner profile monitors at 1.2 GeV [2,3]. Figure 1 shows a schematic diagram of the beam-line components up to the current monitor at 40 MeV.

Here we discuss the simulation from the thermionic gun up to the current monitor at 40 MeV only, where space-charge contributions to the beam dynamics are not negligible. Several computer codes were used in a consistent and integrated fashion for our simulations. We used EGUN [4] to simulate the output from the thermionic gun, SUPERFISH [5] to calculate resonant frequencies and fields in RF cavities, and POISSON [6] to calculate the magnetic fields due to the lenses, solenoids and field-shaping iron. The result from all the codes was used in PARMELA [7] to simulate the beam dynamics up to 40 MeV.

PARMELA calculates charged particle motion in three dimensions with axisymmetric magnetic, RF, and space-charge fields, plus DC quadrupole and dipole fields. Although the particle distributions need not be axisymmetric, axisymmetric space-charge fields are calculated by representing each particle as an axisymmetric ring.

The gun simulations were conducted for a beam with the typical operating parameters of the thermionic gun for high current operation, that is 13×10^{10} electrons per bunch in 2.3 ns FWHM per bunch at 150 KeV. The predicted RMS normalized emittance at the anode is $1.5 \times 10^{-5} \pi$ m-rad with a radius of 6.25 mm at the waist.

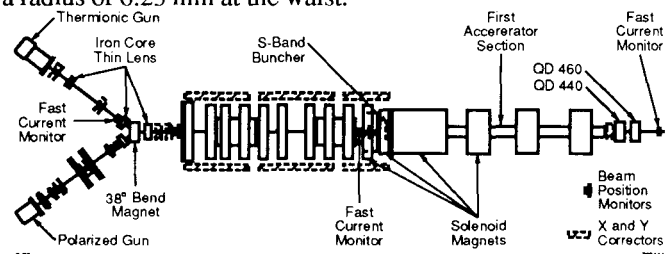


Figure 1. SLC injector beam line up to the fast current monitor at 40 MeV.

*Work supported by Department of Energy contract DE-AC03-76SF00515.

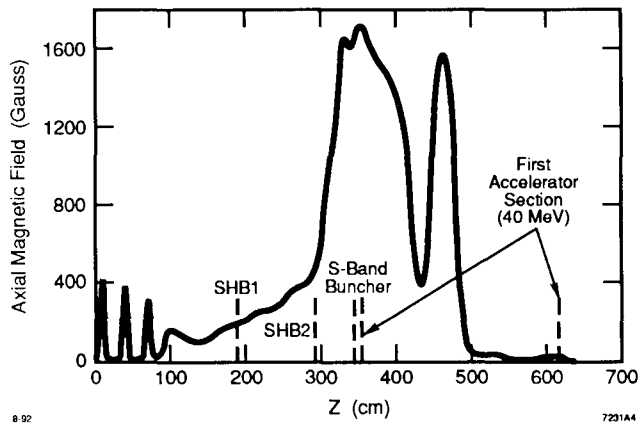


Fig. 2. Axial magnetic field from the cathode to the first quadrupole at 40 MeV.

We then used the beam parameters as predicted by EGUN and the resonant frequencies and fields in the RF cavities as calculated by SUPERFISH as inputs to PARMELA. After a few iterations between POISSON and PARMELA we were able to calculate an axial magnetic field profile for optimum containment of the beam in the radial direction given the actual currents and iron distributions in the magnets. The philosophy we used in optimizing the focusing elements of the injector was to focus as gently as possible. Thus we avoided small waists which, due to space-charge forces, tend to blow up the beam downstream. Figure 2 shows the optimized axial magnetic field as calculated by POISSON, while Figure 3 shows the radial profile of the beam as calculated by PARMELA.

After several more PARMELA runs, we were able to optimize the amplitude and phase of the RF fields in the bunchers and the accelerator to bunch 77% of the total charge from the gun into 20 ps. Figure 4 shows the beam parameters at the current monitor at 40 MeV. The energy of the beam at this point is 40.2 ± 0.7 MeV. The RMS normalized emittance grows from $1.5 \times 10^{-5} \pi$ m-rad at the gun to $8 \times 10^{-5} \pi$ m-rad at the current monitor at 40 MeV. Figure 5 shows the X and Y RMS normalized emittance of the beam. The emittance growth from the gun to the accelerator is due to the increase in space-charge forces and energy spread in the presence of an axial magnetic field as the beam is being compressed in the longitudinal and radial directions. The sharp rise in emittance as the beam goes through the S-band buncher is predominantly due to the time-dependent, radial, RF-defocusing fields, because for bunching purposes the beam is phased with the S-band buncher RF such that it is near the zero-crossing of the longitudinal field, hence the maximum of the radial field. The emittance through the accelerator section is constant because the space-charge effects and the energy-spread percentage are diminished as the beam gains energy, and except for in the first few cells, the beam is now phased near the crest of the longitudinal RF field for acceleration. The

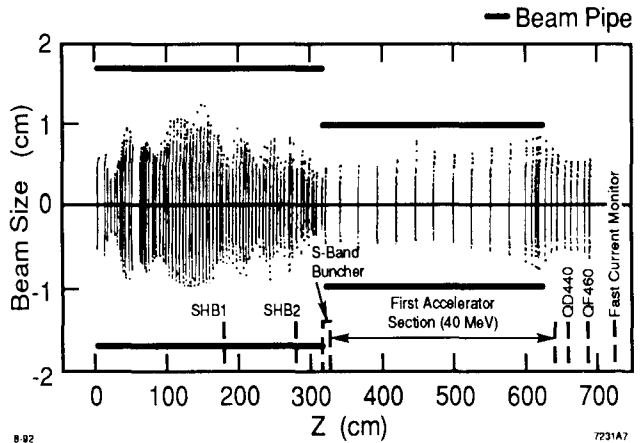


Fig. 3. Beam radial profile from the gun to the fast current monitor at 40 MeV.

slight growth in emittance from the end of the accelerator to the current monitor is due to the beam experiencing the quadrupole magnetic field while it has a rather large energy spread (3.5%). Though the energy spread at 40 MeV seems to be slightly large, it is a small contribution to the energy spread at 1.2 GeV which is dominated by the 20 ps pulse width of the bunch.

Experimental Techniques to Tune the Injector

Once the optimum performance of the injector was achieved in simulation, we had to translate the predicted component settings to the actual hardware and then measure the beam parameters to verify our success.

First we calibrated the actual injector components in order to be able to both set them and to measure the beam parameters. We measured the power in the SHB gaps, and we calibrated the lens and solenoid power supplies to allow us to set them in accordance with our simulations.

We set almost all the injector parameters according to the simulation predictions. These included the gun HV, pulse width and current, the magnetic-element currents, and the buncher RF amplitudes. We were unable to directly set the phases of the bunchers because we do not have a good way to measure the absolute phase of the beam on the RF.

We have observed, both with simulations and in optimizing the hardware settings, that the optimum phase of the bunch on the first SHB RF is not where the center of the bunch passes through the gap at the electric field null, but at about 15° to 20° earlier so that the bunch is somewhat decelerated on the average. Doing this takes advantage of the curvature of the sine function to correct for the fact that velocity is not a linear function of the energy. Using the fast current monitor after the first accelerating station, we were able to count how many S-band RF buckets the beam occupies if both SHBs are off. Then we used SHB 1 to collect most of the beam one bucket (about 20% of 178.5 MHz), later than the middle as observed on the current monitor signal. We then turned on the second SHB

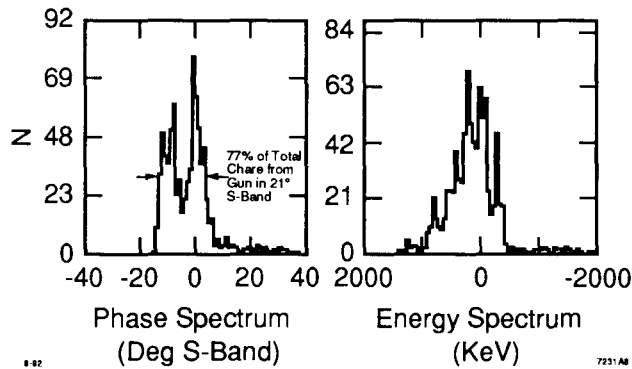


Fig. 4. Electron beam parameters at the fast current monitor at 40 MeV.

buncher and optimized its phase to maximize the signal on the bunch monitor at 40 MeV. To optimize the phase of the S-band buncher with respect to the first accelerator section, we varied the phase of the S-band buncher for every step of phase variation of the accelerating section, while measuring the signal on the bunch monitor. We set the S-band buncher and the first accelerator section phases to the values where the bunch monitor signal was optimized. We then transported the beam from the 40 MeV point to the damping ring, using standard tuning techniques that have been successful on the SLC injector for years and are not the subject of this paper.

We were able to achieve 7×10^{10} electrons in each bunch at the entrance of the damping ring and 5×10^{10} electrons in each bunch out of the damping ring to demonstrate the ability of the injector to meet the SLC requirements. We have measured RMS normalized emittances of $25 \times 10^{-5} \pi$ m-rad at the entrance to the damping ring for 5×10^{10} electrons per bunch out of the damping ring and $10 \times 10^{-5} \pi$ m-rad for 3.5×10^{10} electrons per bunch. The energy spread at 1.2 GeV is 1.5 to 2% for including almost all of the electrons. The intensity jitter of the beam at the entrance of the damping ring is 1.5%.

After optimization of the injector, the beam is about an order of magnitude less sensitive to jitter of the components, because when all the parameters are optimized, all the first derivatives are zero.

Summary

The integrated modeling of the injector using actual locations of the components and using the predicted parameters to set the strengths of these components has allowed us to

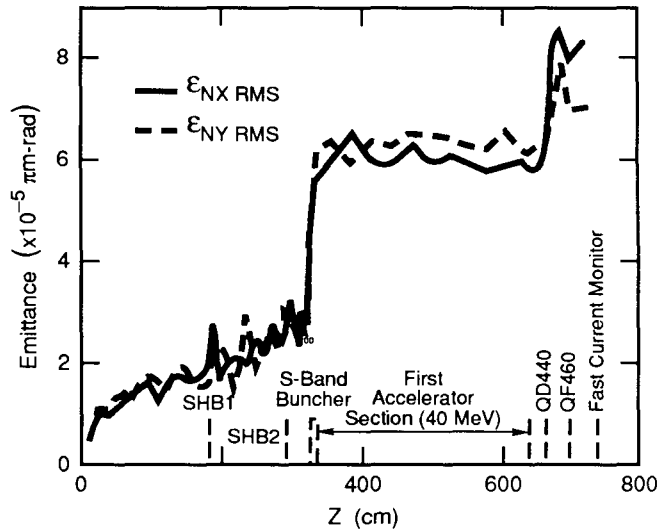


Fig. 5. Normalized emittance from the GUN to the fast current monitor at 40 MeV.

operate the injector to deliver up to 7×10^{10} electrons in each of two bunches to the entrance of the damping ring and 5×10^{10} electrons each bunch out of the damping ring.

References

- [1] M. B. James, R. H. Miller, "A High Current Injector for the Proposed SLAC Linear Collider", *IEEE Trans. Nucl. Sci.*, **NS-28**, (3), 3461 (1981).
- [2] M. C. Ross, "Beam Diagnostics and Control for SLC", *Proc. of the 1987 IEEE Particle Accelerator Conference*, 508, Mar. 16-19, 1987.
- [3] M. C. Ross, "Wire Scanners for Beam Size and Emittance Measurements at the SLC", *Proc. of the 1991 Particle Accelerator Conference*, 1201 (1991).
- [4] W. B. Herrmannsfeldt et. al., "EGUN, Electron Trajectory Program", SLAC-PUB-331 (1988).
- [5] R. Holsinger and K. Halback, "SUPERFISH, a Computer Program for the Evaluation of RF Cavities with Cylindrical Symmetries", *Particle Accelerators*, (7) pp. 212-222 (1976).
- [6] K. Halback, "POISSON Lectures at LBL", 1972 (unpublished).
- [7] K. Crandall and L. Young, "PARMELA: Phase and Radial Motion in Electron Linear Accelerators", Private communication.